by H. Khozyem[1,3], T. Adatte[1], G. Keller[2], A. A. Tantawy[3] and J. E. Spangenberg[4]

The Paleocene-Eocene GSSP at Dababiya, Egypt – Revisited

[1] Institute of Earth Sciences (ISTE), Lausanne University, Switzerland. *E-mail: hassan.saleh.1@unil.ch*
[2] Department of Geosciences, Princeton University, Guyot Hall, Princeton, NJ 08544, USA
[3] Departement of Geology Faculty of science, Aswan University, Aswan, Egypt.
[4] Institute of Earth Surface Dynamics, University of Lausanne, Switzerland

We investigated the Paleocene-Eocene boundary GSSP (Dababiya quarry) near Luxor, Egypt, in two nearby (25m and 50m) sequences based on high-resolution biostratigraphy, lithostratigrapy, mineralogy and geochemistry. Results confirm the many positive aspects of the Dababiya GSSP but also show potentially serious limiting factors: (1) the GSSP is located in the deepest part of a ~200 m wide submarine channel, which limits its use as global type section. (2) Some lithologic units identified at the GSSP are absent or thin out and disappear within the channel and beyond. (3) The P-E boundary is placed at the base of a clay layer above an erosion surface with variable erosion of latest Paleocene and earliest Eocene sediments. (4) The current definition of the P-E boundary as marked by the abrupt onset of the carbon isotope excursion at the base of a clay layer is not supported at the GSSP because 50m to the left the excursion begins gradually 60cm below the P-E boundary and reaches minimum values in the boundary clay. With awareness of these limiting factors and recognition of the gradual onset of the PETM excursion the GSSP can contribute significantly to a more complete understanding of this global warm event.

Introduction

The Paleocene-Eocene Thermal Maximum (PETM) at ~55.9 Ma is one of the most important climatic event of the Cenozoic accompanied by a major $\delta^{13}C$ shift, sudden increase in temperature, diversification calcareous plankton and extinction in benthic foraminifera, followed by temporal diversification and migration of modern mammals (e.g., Kennett and Stott, 1991; Lu and Keller 1995; Pardo et al., 1999; Zachos et al., 2001, 2003, 2005; Berggren and Ouda 2005; Alegret at al., 2005; Alegret and Ortiz, 2007; Westerhold et al., 2009;). McInerney and Wing (2011) summarized the scenarios proposed to explain the PETM including wildfires as a result of burning peat and exposed coal deposits in a dry climate of the Paleocene. Others proposed injection of hydrothermal bodies into organic-rich mudstones of Cretaceous-Paleocene age in the North Atlantic resulting in thermogenic methane release (Westerhold et al., 2009; Svensen et al., 2010), or melting of methane-rich permafrost (DeConto et al. 2010).

Methane release from clathrates is currently the most commonly cited scenario to explain the PETM event. Methane clathrates are stored along the continental margin under stable conditions high pressure and relatively low temperatures. Any change in the physico-chemical conditions of the oceans can result in methane release, including changes in ocean circulation (Dickens et al. 1995), decreased pressure resulting from slope failure (Katz et al. 1999), and change in bottom water temperature due to changes in thermohaline circulation (Bice and Marotzke 2002). On a global scale most studies show an abrupt negative $\delta^{13}C$ shift linked to an abrupt increase in temperature as result of a massive input of greenhouse gases upsetting the carbon cycle in marine and terrestrial ecosystems (Kennett and Stott, 1991; Dickens et al., 1995, Zachos et al., 2001, 2005, 2001; Ernst et al., 2006; John et al., 2008).

In 2003 the International Commission for Stratigraphy (ICS) designated the Dababiya Quarry, located near the Dababiya village, Luxor, Egypt, as the Global Stratotype Section and Point (GSSP) for the Paleocene-Eocene (PE) boundary, which is also marked by the PETM event. The golden spike for the PE boundary was placed in the basal part of the Esna Formation (Dupuis et al., 2003; Aubry et al., 2007) based on the following criteria: (1) the abrupt organic carbon isotope excursion (CIE), (2) extinction of deep-water benthic foraminifera (including *Stensioina beccariiformis*), (3) the transient occurrence of planktonic foraminifera (*Acarinina africana*, *A.sibaiyaensis*, *Morozovella allisonensis*) during the $\delta^{13}C$ excursion, (4) the transient occurrence of the *Rhomboaster* spp. – *Discoaster araneus* (RD) nannofossils assemblage, and (5) an acme of the dinoflagellate *Apectodinium.*

Based on these criteria the Dababiya section was considered the most complete and expanded Upper Paleocene to Lower Eocene sequence and representative of this boundary event globally (Dupuis et al., 2003; Aubry et al., 2007). A lithologic sequence of five distinct beds was identified and believed to be traceable throughout the area and possibly into neighboring countries (Speijer et al., 2000). Subsequently, it was recognized that the basal beds of the GSSP were deposited in a submarine channel with river discharge (Schulte et al., 2011, this study) placing some doubt on the completeness of this section and its value as a global stratotype. This study further evaluates this stratotype section based on (1) the nature and completeness of the sedimentary record, depositional environment and high-resolution biostratigraphy, (2) the nature of the $\delta^{13}C_{Carb}$ and $\delta^{13}C_{org}$ records, and (3) the climate changes before, during and after the PETM event.

Methods

The designated Dababiya GSSP outcrop, which has the most expanded sedimentary record, is not available for sampling because of its limited lateral exposure to a just a few tens of meters. Permission was granted to sample two sections at 50m to left (LSS) and 25m to the right (RSS) of the GSSP (Fig. 1, B and C). A total of 102 samples were collected at 2cm, 5cm, and 10cm sample spacing spanning the Upper Paleocene to Lower Eocene interval.

Biostratigraphy: For foraminiferal analysis about 100gr sediment (from the left side section) was processed per sample by standard methods (Keller et al., 1995). Shell preservation is excellent in carbonate-rich intervals but poor to absent in the PETM excursion interval. Biostratigraphic analysis was performed on >63 mm and 38-63 mm size fractions with quantitative counts of ~300 specimens picked and mounted on cardboard slides for a permanent record and the remaining sample residue searched for rare and zone-defining index species. *For calcareous nannofossils* samples were processed by smear slide preparation from raw sediment samples as described by Perch-Nielsen (1985). Calcareous nannofossils were observed qualitatively with the light microscope at a magnification of 1000×. The taxonomy used is described in Aubry (e.g. 1999) and Perch-Nielsen (1985).

Geochemical and mineralogical analyses: For each sample 25gr of sediment was cleaned and powdered in an agate mortar. After each sample the agate mortar was cleaned three times with deionised water and once with ethanol, and then air-dried to avoid sample contamination. Powdered samples were analysed for bulk rock mineralogy and stable isotopes ($\delta^{13}C_{car}$, $\delta^{13}C_{org}$) at the Institute of Earth Sciences (ISTE) at Lausanne University, Switzerland.

For XRD mineralogy, whole rock and clay mineral analyses, samples were prepared following the procedures of Kübler (1987) and Adatte et al. (1996). The semi-quantification of whole-rock mineralogy is based on XRD patterns of random powdered samples by using external standards with an error margin between 5 and 10% for the phyllosilicates and 5% for grain minerals.

Geological setting and lithostratigraphy

The Dababiya GSSP section is located on the eastern side of the upper Nile Valley 35 km southeast of Luxor City (25°30' N, 32°31' Fig.1A). Four lithostratigraphic formations (Fm) are exposed in the area: the Dakhla Fm. at the base is a greenish calcareous shale, above is the marly limestone to chalk of the Tarawan Fm., followed by the green-gray to dark-gray shale of the Esna Fm. and ending at the top with the limestones or flint of the Thebes Fm. Dupuis et al. (2003) subdivided the Esna Fm. into three main units (Esna-1, Esna-2, and Esna-3) based on carbonate contents. Only Esna-1 and Esna-2 are exposed at the GSSP (Figs. 2, 3). The P/E boundary is placed in the lower part of the Esna Fm. between Esna-1 and Esna-2, about 7m above the Tarawan Formation. Five distinct beds in Esna-2 mark the GSSP PETM interval (Dupuis et al., 2003). At the base of Esna-2, Bed-1 consists of 0.63m of dark laminated, non-calcareous clay with a few phosphatic coprolites at the base. The overlying Bed-2 consists of 0.5m of brown shale with coprolites and low carbonate content. Bed-3 is a 0.84m-thick shale, cream-colored, laminated and phosphatic. Bed-4 is a 0.71m-thick gray shale with high carbonate content, and Bed-5 consists of 1m-thick grey marl to marly limestone (Fig. 2).

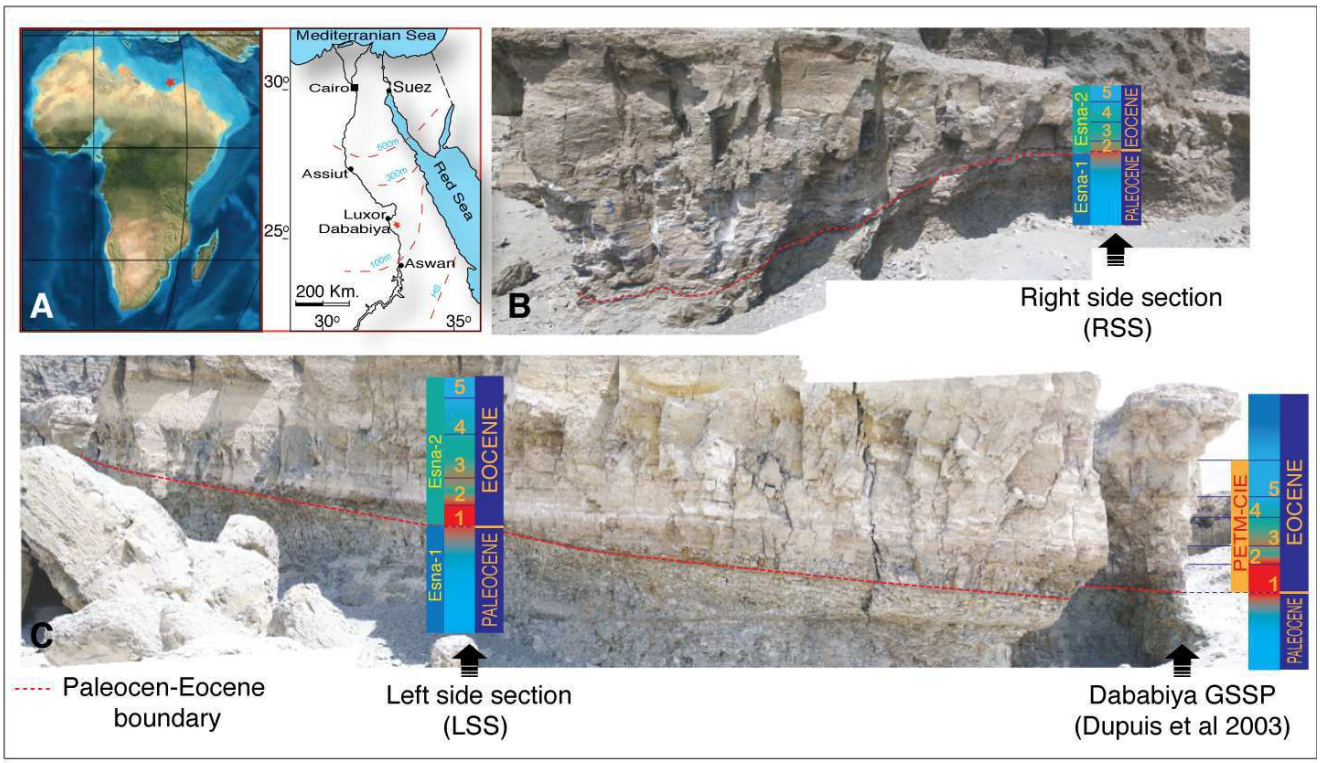

Figure 1. A: Location of the Dababiya GSSP. B and C: Field photographs show the lithology across the 25 m from the GSSP to the right side section (RSS) and the 50 m to the left side section (LSS). Note the sharp thinning out of the sedimentary units to the right and more gradual thinning out to the left of the GSSP marks a channel deposit.

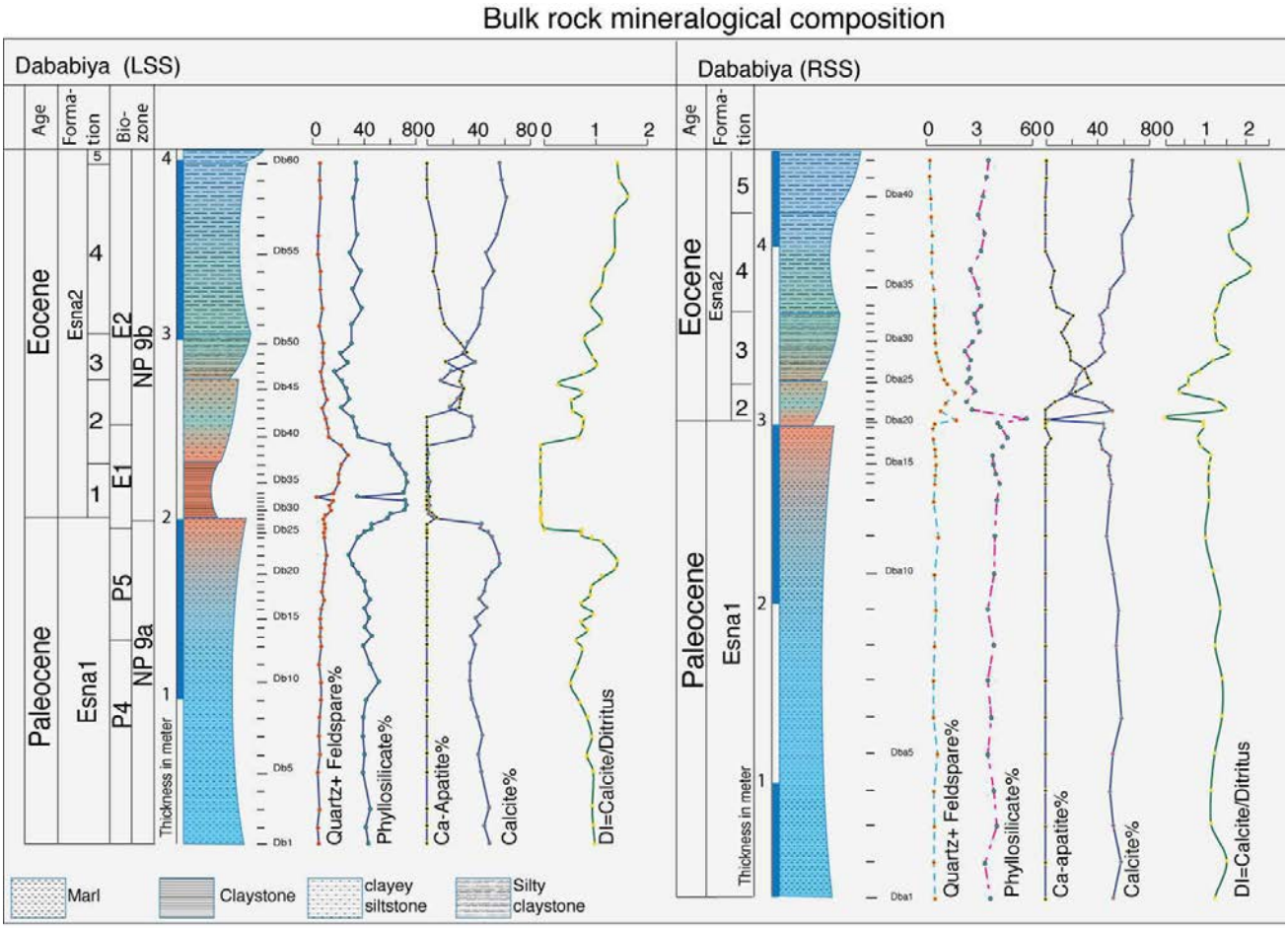

Figure 2. Vertical distribution of bulk rock mineralogical data in the sections to the left (LSS) and right (RSS) of the GSSP. Note the differences in bulk rock compositions in these channel deposits reflect the absence of the lowermost Eocene sediments from the RSS.

At 50m to the left of the GSSP the Dababiya left side section (LSS) was sampled. The section consists of the late Paleocene marl to marly shale of Esna-1, a well-defined sequence boundary (SB) and the overlying early Eocene Esna-2 units (Figs. 2, 3B). Esna-2 units are significantly reduced to the left and right sides from the GSSP location reflecting the submarine channel morphology. Following Dupuis et al. (2003) we divide Esna-2 into five beds with the following thicknesses and lithological characteristics: Bed-1 (0.32m) and Bed-2 (0.48m) consist of slity claystone with anhydrite layers. Bed-3 (0.24m) is a silty marl with phosphatic nodules and anhydrite. Bed-4 (1.0m) consists of marl to marly limestone (Fig. 2). Only the basal 5cm was recovered from Bed-5.

At 25m to the right of the GSSP the Dababiya right side section (RSS) was sampled with the same lithologies as at the LSS, except that Bed-1 is absent and possibly also the lower part of Bed-2, which is only 0.24m thick (Fig. 3B), as also suggested by mineralogic data including the absence of one of the four anhydrite layers present in LSS (Fig. 2, discussed below). Bed-3 (0.4m) consists of silty clay with phosphatic nodules, Bed-4 (0.6m) is marl and Bed-5 consists of a 0.4m thick marly limestone (Fig. 2).

Results

Bulk rock mineralogy

At Dababiya LSS, bulk rock components in the interval below the PETM (samples 1 to 27) indicate marls with a low detrital index (DI 1.15) and average 42.70% calcite, 40.65% phyllosilicates, 6.93% quartz, 0.37% anhydrite (Ca-apatite is absent, Fig. 2). The sequence boundary (SB) marks the base of the PETM and a sharp decrease in calcite (5.44%) coincides with increased phyllosilicate (57.74%), quartz (8.21%), anhydrite (7.09%), and Ca-apatite (7.48%). The detrital index is relatively high (DI 1.3). Also present are goethite (1.64%), K (1.76%) and Na feldspar (3.04%).

In Esna-2 three distinct intervals mark Beds 2-5. Bed-1 to base Bed-2 (samples 29-39) shows an abrupt increase in phyllosilicate (64.77%), quartz (16.75%), goethite (1.26%), and anhydrite (11.7%) (Fig. 2). In contrast, K- and Na- feldspar are low and calcite nearly zero (0.82%) and low Ca-apatite (0.56%). In the middle of Bed-2 (samples 40-42), sharply increased calcite (34.48%) correlates with decreased other bulk rock contents and disappearance of Ca- apatite. Upper Bed-2 and Bed-3 (samples 43-50) contain maximum Ca-apatite (25.56%) coincident with increasing anhydrite and decreasing other minerals, though calcite remains relatively high (24.27%). Bed-4 shows the return to marl composition (average: calcite 49.93%, phyllosilicate 33.2%, Ca-apatite 5.81%, quartz 5.54%, anhydrite 1.08%).

RSS is similar to LSS except that Bed-1 and the lower part of Bed-2 are missing (Fig. 2). Below the P/E boundary marls contain relatively high phyllosilicate (38.76%), and calcite (49.74%) and low quartz (5.34%). An abrupt change at the P/E boundary (Bed-2, sample 21) shows increased phyllosilicate (57.09%) and quartz (17.35%),

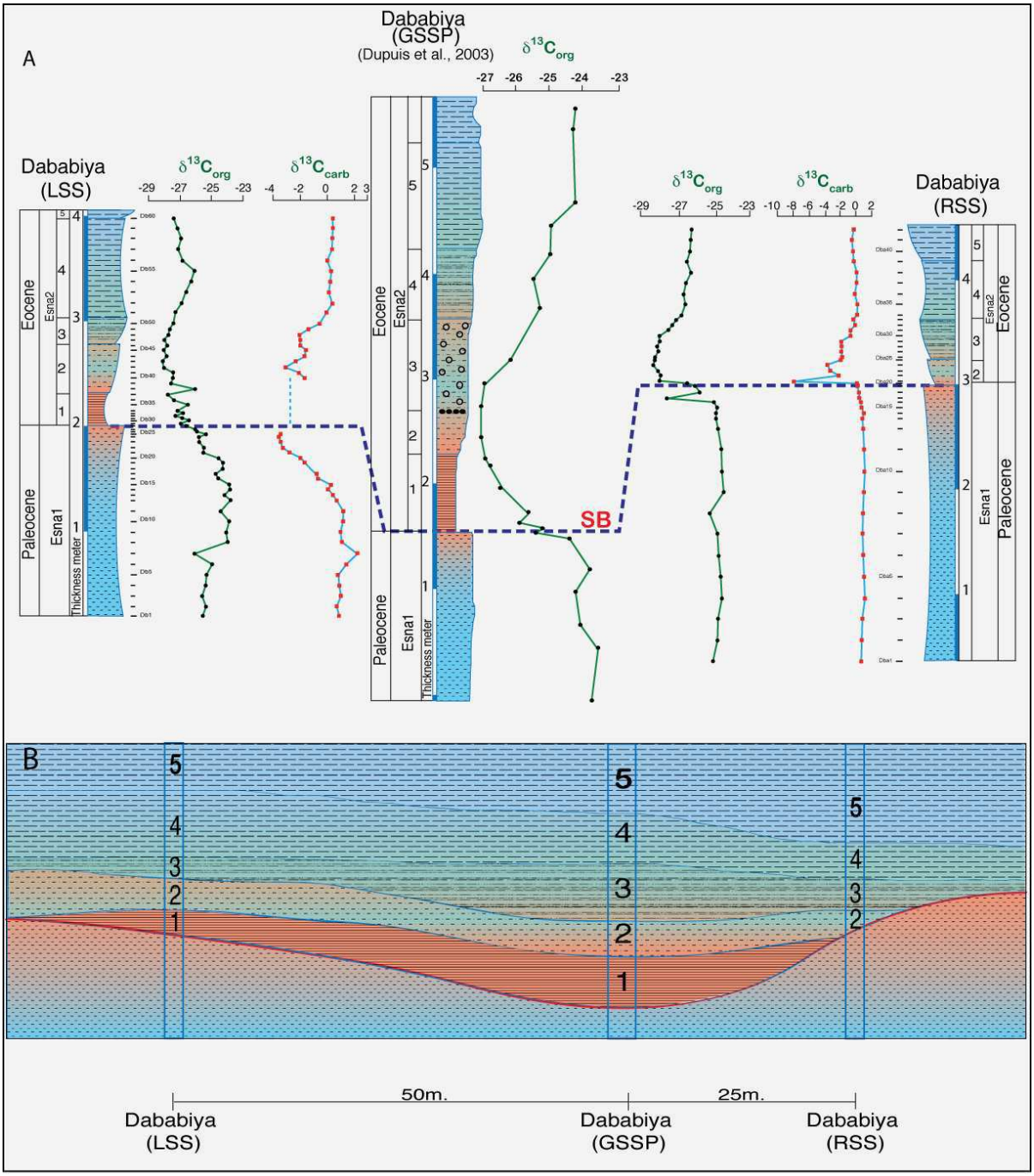

Figure 3. A. Correlation of the LSS and the RSS with the published Dababiya GSSP (Dupuis et al., 2003) based on both organic Carbon isotopes, and new data obtained for inorganic carbon isotopes. Both $\delta^{13}C_{Carb}$ and $\delta^{13}C_{org}$ in the LSS show gradual decreases starting 60cm below the SB. The $\delta^{13}C_{Carb}$ CIA-minimum coincides with the SB whereas the $\delta^{13}C_{org}$ CIA-minimum is in the upper third of bed-2. B. Diagram illustrating the lateral disappearance of beds 1 and 2 on either sides of the main GSSP marks deposition in asymmetric channel. See photo illustration in Fig. 1B,C.

and sharply decreased calcite (1.64%). From the upper Bed-2 into the middle of Bed-3 (samples 22-31) calcite increases to 35.27% and phyllosilicate and quartz decrease to 25.13% and 9.33%, respectively. In Beds 4 and 5 (samples 32-42, Fig. 2), all bulk rock components return to the marl composition observed below the P/E boundary.

Stable isotopes

The Dababiya LSS and RSS were measured for bulk rock carbonate isotopes ($\delta^{13}C_{carb}$) and organic carbon isotopes ($\delta^{13}C_{org}$) and compared with the $\delta^{13}C_{carb}$ of the GSSP section (Dupuis et al., 2003). At LSS the upper Paleocene (samples 1-15) shows relatively steady $\delta^{13}C_{carb}$ values around 1‰ (except for a single point of 2.2‰, Fig. 3A). In the 50cm below the PE boundary (samples 16-27) $\delta^{13}C_{carb}$ values gradually decrease to -3.5‰. The PETM corresponding to Bed-1 and base of Bed-2 is carbonate poor yielding no $\delta^{13}C_{carb}$ data. From Bed-2 to the middle of Bed-3 $\delta^{13}C_{carb}$ values remain low at around -2‰, then rapidly increase to about 0‰ near the base of Bed-

4 and reaching 0.39‰ at the top of the section (Fig. 3A).

Organic carbon isotopes show similar trends. In the lower part of Esna-1 $\delta^{13}C_{org}$ values are around -25.8‰, then increase to -23.8‰ (sample 8) and gradually decrease to the minimum values between -27 ‰ and -28 ‰ in the PETM interval (Beds-1 and 2). A gradual increase in Bed-3 reaches maximum values of -26.1‰ in the middle of Bed-4 (sample 55) then gradually decreases at the top of the section.

Dababiya RSS differs significantly from the LSS section due to the erosional disconformity that marks the P/E boundary (Fig. 3A). Paleocene values of both $\delta^{13}C_{org}$ and $\delta^{13}C_{carb}$ are steady through Esna-1 with a sharp negative excursion at the P/E boundary. This indicates that the gradual decrease observed in the LSS section is missing due to erosion as also indicated by the missing Bed-1 of the basal Paleocene. The $\delta^{13}C_{org}$ and $\delta^{13}C_{carb}$ values average of -28 and -2.41‰, respectively, above the erosion surface in Beds-2 and 3 (samples 20-31) and are similar to the equivalent interval in the LSS. In Beds 4 and 5 $\delta^{13}C_{org}$ (-26.7) and $\delta^{13}C_{carb}$ (0.5‰) values return to nearly pre-P/E boundary values (-25.3 and 0.89‰).

Biostratigraphy

Planktic foraminiferal and calcareous nannofossil biostratigraphy of the more complete Dababiya LSS shows major turnovers across the PETM interval (Fig. 4). Planktic foraminifera span biozones P4c, P5, E1 and E2 with an estimated time span of 2 m.y. (54.5-56.5Ma, Olsson et al., 1999; Pearson et al., 2006). Zone P4c marks the base of the section (samples 1-12) as indicated by the disappearance of the index species *Globanomalina pseudomenardii*. This assemblage is dominated by *Igorina tadjjikistanensis, Acarinina soldadoensis, Subbotina hornibrooki, Morozovella acuta and M. aequa*.

The interval from the extinction of *Gl. pseudomenardii* to the first appearance of *Acarinina sibaiyaensis* marks zone P5 and the top of the Paleocene. At Dababiya LSS this 62cm thick interval corresponds to the gradual decrease in $\delta^{13}C_{org}$ and $\delta^{13}C_{carb}$ values, and experienced a 40% increase in species diversity (from 21 to 35 species) and decreased abundance of the dominant zone P5 species. Most common among the newly appearing species are *Igorina broedermanni, I. lodoensis, Globanomalina luxorensis, Gl. australiformis, Gl. chapmani, Gl. planoconica,* and *Morozoevella gracilis*.

Acarinina sibaiyaensis, which marks the base of zone E1, first appears just below the 42 cm thick barren clay interval of Bed-1 (samples 25-26). A good assemblage of the transient PETM fauna dominated by *A. sibaiyaensis* and *A. africana* and the first appearances of *A. africana, Morozovella allisonensis*, and the zone E2 index species *Pseudohastigerina wilcoxensis* occurs in a 5 cm interval between the barren clay below and the slightly calcareous clay above (Fig. 4). The upper clay (35cm, upper Bed-2 and Bed-3 corresponds to the upper part of the PETM. Bed-4 contains a diverse and well-preserved zone E2 assemblage (*P. wilcoxensis* and *M. velascoensis*) dominated by *Planorotalites pseudoscitula, Morozovella acuta, I. lodoensis, I broedermanni, A. esnaensis, A. eshnehensis).* The return of this thriving assemblage coincides with the recovery of the $\delta^{13}C_{org}$ and $\delta^{13}C_{carb}$ values after the PETM.

The calcareous nannofossil assemblage is moderately diversified, and the preservation varies from poor to moderate, except for the dissolution interval (devoid of nannofossils) that spans Bed-1 and the lower part of Bed-2. Below the barren interval, nannofossil diversity averages about 16 species, whereas above it both abundance and diversity sharply decrease to about 8 species and dissolution resistant taxa dominate (e.g. *Discoaster spp, Coccolithus pelagicus*) along with reworked forms. Nannofossil diversity increases gradually

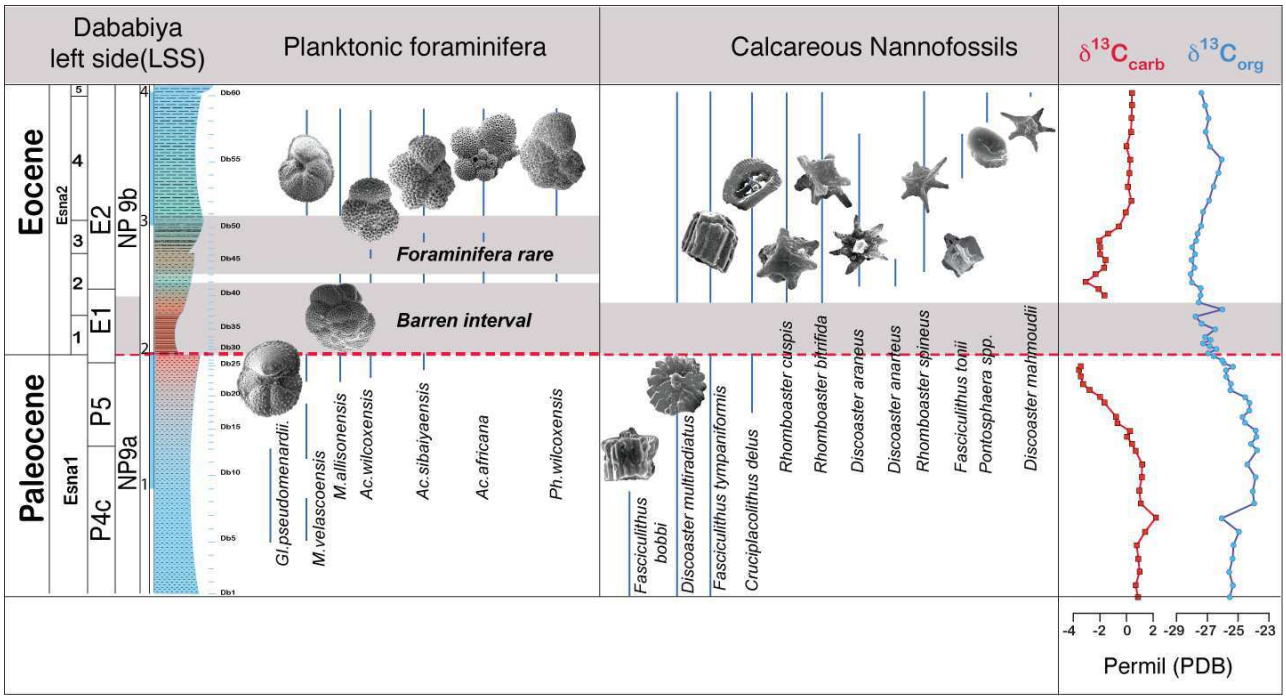

Figure 4. Carbon isotopes ($\delta^{13}C_{org}$ and $\delta^{13}C_{carb}$) and selected species ranges of planktic foraminifera and calcareous nannofossil species at 50 m to the left of the Dababiya GSSP. Note that a reduction in species richness in the late Paleocene is offset by a few new species during the gradual decrease in carbon isotopes and this evolutionary trend increased during the gradual recovery in carbon isotopes in the early Eocene.

parallel to the CIE and reaches a maximum at the base of Bed-5 (Fig. 4).

The calcareous nannofossil turnover spans subzones NP9a and NP9b (e.g., Martini, 1971; Aubry 1995, 1999). The first appearance of *Discoaster multiradiatus* defines the base of Zones NP9 of Martini (1971) whereas *Fasciculithus bobbi* disappears consistently near the middle of subzone NP9a (sample 9) and *F. alanii* near the top (Fig. 4, Perch-Nielsen, 1985; Aubry, 1999). Most species disappear at the P/E transition, and only F. tympaniformis survives and becomes extinct in the lowermost Eocene. *Fasciculithus tonii* last occurs in the upper Bed-4 (sample Db57) this species must be reworked here, because it is one of the Paleocene large fasciculthus that disappear at the onset of CIE-PETM and *F. tympaniformis* at the base of Bed-5 (sample 60), as also observed in the Atlantic, Pacific and Tethys oceans (Monechi et al., 2000; Raffi et al., 2005; Tantawy, 2006; Agnini et al., 2007).

The base of Subzone NP9b was defined based on the first appearances of *Campylosphaera eodelus* and *Rhomboaster spp* (Okada and Bukry, 1980), or alternatively the simultaneous first appearances of *R. calcitrapa*, *R. spineus*, *D. araneus* and *D. anartios* (Aubry et al., 2003). At Dababiya the NP9a/NP9b transition coincides with the PETM dissolution interval, which is followed by the first appearance of *Rhomboaster cuspis* and *R. bitrifida* (sample 40), *D. araneus* and *D. anarteus* (sample 41), whereas *C. eodelus* appears earlier in NP9a (sample 18) and *R. spineus* later in NP9b (Fig. 4) as also observed in the southeast Atlantic (Agnini et al., 2007) and Kharga Oasis, Western Desert, Egypt (Tantawy 2006). Other taxa first appear above the dissolution interval, including poorly preserved *Pontosphaera plana* in the upper part of Bed-4 (sample 58) and *Discoaster mahmoudii* at the base of Bed-5 (sample 60, Fig. 4).

Discussion and Conclusions

The most important criterion for any GSSP is a continuous sedimentation record. In the primary analysis leading to the designation of the Dababiya section as GSSP, the sedimentation record was considered expanded and complete (Dupuis et al., 2003; Ouda, 2003; Aubry et al., 2007). This conclusion was supported by an expanded and gradually changing carbon isotope curve across the PETM. Subsequently, Schulte et al. (2011) observed that the deposition of the GSSP occurred in a submarine channel, which introduced some doubts as to the viability of Dababiya as a global representative of the PE boundary event. Our study confirms deposition in a submarine channel, but also determined significant lateral variations in lithology and mineralogy within 25m and 50m of either side of the GSSP suggesting erosion and/or non-deposition. We discuss these observations and their implications for the viability of Dababiya as GSSP.

How complete is the GSSP?

Lithostratigraphy

The Paleocene-Eocene boundary at the Dababiya GSSP is placed at a sequence boundary (SB) that marks a change in lithology from hemipelagic marine to sediments enriched in fluvial discharge (Schulte et al., 2011). This lithologic change is characterized by: (1) increased detrital components (quartz, phyllosilicates and feldspar) and decreased carbonate content. The latter may be linked to carbonate dissolution and/or dilution due to increased detrital input (Fig. 2). (2) The thickness of Bed-1 is variable: at the maximum in the main GSSP outcrop, reduced to half the thickness at 50m to the left (LSS) and absent at 25m to the right (RSS). (3) Above the sequence boundary, the change in the vertical distribution of the bulk rock compositions from the LSS to the RSS outcrops shows persistent increases in phyllosilicates and quartz, the presence of feldspar and minimum values in calcite (Fig. 2). The bulk rock composition at the RSS outcrop shows abrupt changes at the P/E boundary as quartz, feldspar, and phyllosilicates increase and calcite decreases within a 5cm thick interval above the SB. This abrupt change in the bulk rock composition marks the absence of lowermost Eocene sediments from the RSS outcrop due to erosion linked to the existing paleorelief. (4) Variation in Ca-apatite is another indicator of erosion and/or variable sedimentation. In the LSS outcrop Ca-apatite increased 60cm above the SB whereas in the RSS outcrop this increase is observed just above the SB. This suggests that at least 60cm is missing at the RSS compared with the LSS outcrop and about 80cm missing compared with the GSSP (including Bed-1 and part of Bed-2, Fig. 3, 3B).

Based on field observations and variations in bulk rock compositions, we conclude that the lower part of the Dababiya GSSP section (Bed-1 and Part of Bed-2) was deposited in a submarine channel. This channel extended at least 25m to right of the GSSP and about 150m to the left with maximum width of about 200m. The sequence boundary (SB) marks erosion and/or condensed sedimentation, which varies in the three outcrops as evident in the presence or absence of lithologic units particularly early Eocene Beds-1 and 2. The maximum depth of this channel-fill above the SB at the main GSSP outcrop is about 0.88m (Bed-1 to middle part of Bed-2) and missing at RSS, as also indicated by the absence of the 0.60m thick Ca-apatite rich interval of the LSS outcrop. In contrast, the LSS outcrop is more complete though condensed compared with the GSSP (Fig. 2).

Isotope stratigraphy

At Dababiya the carbon isotope records of three closely spaced sections over a distance of just 75m yield further confirmation of the variable erosion pattern at the GSSP location. Dupuis et al.'s (2003) $\delta^{13}C_{org}$ values for the Dabbabiya GSSP can be divided into three main parts: (1) a rapid decrease 10 cm below Bed-1 and the SB where the P/E boundary is placed followed by gradually decreasing values through Bed-1; (2) minimum values persist through Bed-2 into the lower 1/3 of Bed-3; (3) a gradual increase in Bed-3 to the middle of Bed-5 reaching background values (Fig. 3).

The two sections analyzed to the right and left of the GSSP show similarities and differences. The most comparable is the LSS outcrop where carbon isotope analysis permits the same subdivisions as the GSSP but with important differences. Most important is the gradual decrease in $\delta^{13}C_{Carb}$ and $\delta^{13}C_{org}$ in the uppermost Palaeocene spanning about 60cm below the SB (Fig. 3A). This latest Paleocene interval is not present at the GSSP or the RSS outcrops where both $\delta^{13}C_{org}$ and $\delta^{13}C_{Carb}$ curves shift abruptly at the SB. This suggests that a minimum 60 cm is missing at the top of the Paleocene at the GSSP and probably more at the RSS outcrop. Isotope stratigraphy also confirms the absence of the basal Eocene (Bed-1 and half of Bed-2) at the RSS outcrop. This is evident in the $\delta^{13}C_{Carb}$ values of the upper Bed-2 at LSS that mirror similar values in the upper Bed-2 directly overlying the SB horizon at the RSS outcrop. In the early Eocene $\delta^{13}C_{org}$ curves

at LSS and GSSP are very similar with minor differences due to the lower sediment accumulation rate and higher sample resolution at LSS compared with the GSSP.

Implications for the GSSP

The idea of the GSSP record is to have a single locality and section were all the best characteristics of a given boundary event can be observed and taken as representative of coeval sequences worldwide. Ideally the GSSP should have a continuous sedimentation record with no discernable interruptions due to current erosion or tectonic disturbance, the fossil content should be abundant and well preserved and the lithology should have characteristic features that permit easy identification in the field at the GSSP as well as in coeval sequences globally. The Dababiya GSSP satisfies these qualifications in most parts, including excellent outcrops, well-preserved fossil records (except for the PETM clay layer), easily identifiable lithostratigraphic units (at least for the area), characteristic mineralogical and geochemical contents, and globally representative carbon isotope signals (Dupuis et al., 2003; Zachos et al., 2001). Based on all these characteristics, the Dababiya section was deemed to be the best choice for the Paleocene-Eocene boundary event and designated the GSSP (Aubry et al., 2007).

No GSSP is perfect and no single locality can be representative of all coeval sedimentary sequences globally. Some adjustments have to be made for local characteristics whether at the GSSP locality or elsewhere. The Dababiya GSSP is no exception. Our research based on lithostratigraphy, stable isotope stratigraphy and biostratigraphy demonstrates a few problems: (a) the chosen GSSP is located in a submarine channel that is asymmetric and about 200m wide. (b) The P/E boundary placed at the base of the clay layer is a sequence boundary that marks the channel along with variable erosion. (c) The critical PETM Beds-1 to 4 are of varying thickness and/or absence due to erosion, including absence of the latest Paleocene at the GSSP and RSS outcrops and early Eocene erosion at RSS (Bed-1 to middle Bed-2. Fig. 3A) making long-distance correlation problematic even within the area let alone globally.

All these factors present some problems for the Dababiya GSSP, but how serious are they? When the two new sections (RSS, LSS) plus the GSSP are viewed in their lateral positions in the submarine channel (Fig. 3A, B), erosion at the sequence boundary is greatest (total of 1.2m) at the RSS outcrop encompassing both latest Paleocene and earliest Eocene. At the GSSP outcrop just 25m to the left erosion primarily affects the latest Paleocene (total of about 0.60m). At LSS just 50 m further to the left of the GSSP, erosion appears to be minimal as observed by the gradual change of the carbon isotope curves. However, the overall rate of sediment accumulation is highest at the GSSP, as would be expected with its location in the deepest part of an asymmetric submarine channel.

Erosion at the P/E sequence boundary is thus the most negative aspect of the GSSP. On the positive side erosion appears limited in some sections and the overall shape of the carbon isotope curves (both $\delta^{13}C_{Carb}$ and $\delta^{13}C_{org}$) show gradual changes approaching the P/E sequence boundary with minimum values reached in the clay layer and followed by a gradual increase to pre-PETM values. How common are these gradual $\delta^{13}C$ changes across the PETM? Although most PETM records show abrupt changes, more gradual long-term decreases in $\delta^{13}C_{Carb}$ and $\delta^{13}C_{org}$ were observed at ODP site 690 (Bains et al., 1999) and in pedogenic carbonate from Polecat Bench, Wyoming (Bowen et al., 2001). This suggests that the Dababiya GSSP may indeed be among the more complete and expanded records despite the SB erosion and can serve as reference section for the global record.

Acknowledgements

We are grateful to the Egyptian ministry of state for environmental affairs and the president of the International Committee of Stratigraphy (ICS) for providing the necessary permission and official access to the GSSP site for sampling. We thank S. Gardin and A. Sahni for their constructive reviews. This study was conducted at the University of Lausanne. Funding was provided to HK by the Egyptian ministry of higher education (mission No.001/013/104). Partial support was received from the University of Lausanne and the US National Science Foundation NSF OISE-0912144.

References

Adatte, T., Stinnesbeck, W., and Keller, G., 1996, Lithostratigraphic and mineralogic correlations near K/T boundary clastic sediments in northern Mexico: Implication for origin and nature of deposition: Geological Society of America, Special Papers, v. 307, pp. 211–226

Agnini, C., Fornaciari, E., Rio, D., Tateo, F., Backman, J., and Giusberti, L., 2007, Responses of calcareous nannofossil assemblages, mineralogy and geochemistry to the environmental perturbations across the Paleocene/Eocene boundary in the Venetian Pre- Alps: Marine Micropaleontology, v.63, pp. 19–38.

Alegret, L., and Ortiz, S., 2007, Global extinction event in benthic foraminifera across the Paleocene/Eocene boundary at the Dababiya Stratotype section: Micropaleontology, v. 52, no. 5, pp. 433-447.

Alegret, L., Ortiz, S., Arenillas, I., and Molina, E., 2005, Palaeoenvironmental turnover across the Palaeocene/Eocene boundary at the Stratotype section in Dababiya (Egypt) based on benthic foraminifera: Terra Nova, v. 17, no. 6, pp. 526–536.

Aubry, M.-P., Berggren, W.A., Van Couvering, J.A. , Ali, J., Brinkhuis, H., Cramer, B., Kent, D.V., Swisher, III, C.C., Gingerich, P.R., Heilmann-Clausen, C., Knox, R.W.O'B., Laga, P., Steurbaut, E., Stott, L.D., and Thiry, M, 2003, Chronostratigraphic Terminology at the Paleocene/Eocene Boundary: In Wing, S.L., Gingerich, P.D., Schmitz, B., and Thomas, E., eds., Causes and Consequences of Globally Warm Climates in the Early Paleogene: Boulder, Colorado, GSA Special Paper 369, Chapter 35, pp. 551–566.

Aubry, M.-P., Berggren, W. A., Cramer, B., Dupuis, C., Kent, D. V., Ouda, K., Schmitz, B., And Steurbaut, E., 1999, Paleocene/Eocene Boundary Sections in Egypt. In Ouda, K., Ed., Late Paleocene-Early Eocene Events from North Africa to the Middle East, Symposium. First International Conference on the Geology of North Africa, pp.1-11.

Aubry, M.-P., Ouda, K., Dupuis, C., Berggren, W.A., Van Couvering, J.A., Members of the Working Group on the Paleocene/Eocene Boundary, 2007, The Global Standard Stratotype-section and Point (GSSP) for the base of the Eocene Series in the Dababiya section (Egypt): Episodes, v.30 no.4, pp. 271–286.

Bains, S., Corfield, R. M., and Norris, R. D., 1999, Mechanisms of climate warming at the end of the Paleocene: Science, v. 285, pp. 724-727.

Berggren, W., and Ouda, K., 2005. Upper Paleocene-lower Eocene planktonic foraminiferal biostratigraphy of the Dababiya section, Upper Nile Valley (Egypt): Micropaleontology, v. 49, pp. 61-92.

Bice, K. L., and Marotzke, J., 2002, Could changing ocean circulation have destabilized methane hydrate at the Paleocene/Eocene boundary? Paleoceanography, v.17, no. 2, pp.1018

Bowen, G.J., Koch, P.L., Gingerich, P.D., Norris, R.D., Bains, S., Corfield, R.M., 2001. Refined isotope stratigraphy across the continental Paleocene-Eocene boundary at Polecat Bench in the northern Bighorn Basin: University of Michigan: Papers on Paleontology, v.33, 73-88.

DeConto, R., Galeotti, S., Pagani, M., Tracy, D.M., Pollard, D. and Beerling, D.J., 2010, Hyperthermals and orbitally paced permafrost soil organic carbon dynamics: Presented at AGU Fall Meet., Dec. 13–17, San Francisco (Abstr. PP21E-08)

Dickens, G. R., O'Neil, J. R., Rea, D. K., and Owen, R. M., 1995, Dissociation of oceanic methane hydrate as a cause of the carbon isotope excursion at the end of the Paleocene: Paleoceanography, v.10, pp. 965-971.

Dickens, G., 2001, Carbon addition and removal during the Late Palaeocene Thermal Maximum: basic theory with a preliminary treatment of the isotope record at ODP Site 1051, Blake Nose, in: D. Kroon, R.D. Norris, A. Klaus (Eds.), Western North Atlantic Palaeogene and Cretaceous Palaeoceanography: Geological Society of London, Special Publication, v.183, pp. 293–305.

Dupuis, C., Aubry, M.-P., Steurbaut, E., Berggren, W.A., Ouda, K., Magioncalda, R., Cramer, B.S., Kent, D.V., Speijer, R.P., and Heilmann-Clausen, C., 2003, The Dababiya Quarry section: lithostratigraphy, clay mineralogy, geochemistry and paleontology. In: Ouda, K., Aubry, M.-P. (Eds.), The Upper Paleocene–Lower Eocene of the Upper Nile Valley: Part 1.Stratigraphy: Micropaleontology, v. 49, pp. 41–59.

Ernst, S.R., Guasti, E., Dupuis, C., and Speijer, R.P., 2006, Environmental perturbation in the southern Tethys across the Paleocene/Eocene boundary (Dababiya, Egypt): foraminiferal and clay mineral records: Marine Micropaleontology, v. 60, no.1, pp.89–111.

Gavrilov, Y.O., Shcherbinina, E.A., and Oberhänsli, H., 2003, Paleocene-Eocene boundary events in the northeastern Peri-Tethys: Geological Society of America, Special Publication, v. 369, pp.147–68

John, C. M., Bohaty, S. M., Zachos, J. C., Gibbs, S., Brinkhuis, H., Sluijs, A., and Bralower, T., 2008, Impact of the Paleocene-Eocene thermal maximum on continental margins and implications for the carbon cycle in near-shore environments: Paleoceanography, v. 23, p. PA2217.

Katz, M.E., Pak, D.K., Dickens, G.R., and Miller, K.G., 1999, The source and fate of massive carbon input during the Latest Paleocene Thermal Maximum: Science, v. 286, pp.1531–33

Keller, G., Li, L., and Macleod, N., l995, The Cretaceous/Tertiary boundary stratotype section at El Kef, Tunisia: How catastrophic was the mass extinction? Palaeogeography, Palaeoclimatology, Palaeoecology, v. 119, pp. 221-254.

Kennett, J.P., and Stott, L.D., 1991, Abrupt deep-sea warming, palaeoceanographic changes and benthic extinctions at the end of the Paleocene: Nature, v. 353, pp.225–229

Kübler, B., 1987, Cristallinité de l'illite: méthode normalisées de préparation de mesure, méthode automatique normalisées de mesure: Cahiers de l'Institut de Géologie, Series AX no. 3.1 and 3.2.

Lu, G.Y., and Keller, G., 1995, Planktic foraminiferal faunal turnovers in the subtropical Pacific during the Late Paleocene to Early Eocene: Journal of Foraminifera Research, v. 25, pp. 97–116.

Martini, E., 1971. Standard Tertiary and Quaternary calcareous nannoplankton zonation, in FARINACCI, A. (ed.), Proceedings of the Second Planktonic Conference. Roma, Italy, Tecnoscienza, p. 739-785.

McInerney, F. A., and Wing, S. L., 2011, The Paleocene–Eocene Thermal Maximum: A perturbation of carbon cycle, climate, and biosphere with implications for the future: Annual Review in Earth Planetary Science, v. 39, pp. 489–516.

Monechi, S., Angori, E., and Speijer, R.P., 2000, Upper Paleocene biostratigraphy in the Mediterranean region: Zonal markers, diachronism, and preservational problems. GFF. Geologiska Föreningens, Stockholm Förhandligar, v.122, pp.108-110.

Okada, H., and Bukry, D., 1980., Supplementary modification and introduction of code numbers to the low-latitude coccolith biostratigraphic zonation (Bukry, 1973; 1975): Marine Micropaleontology, v. 5, pp. 321–325

Olsson, R.K., Berggren, W.A., Hemleben, C., and Huber, B.T., 1999, Atlas of Paleocene planktonic foraminifera - online version. Smithsonian Contributions to Paleobiology, v. 85, pp. 1-252

Ouda, K., and Berggren, W.A, 2003, Biostratigraphic correlation of the Upper Paleocene–Lower Eocene succession in the Upper Nile Valley: a synthesis: Micropaleontology, v. 49, pp. 179–212.

Pardo, A., Keller, G., and Oberhänsli, H., 1999, Paleoecologic and paleoceanographic evolution of the Tethyan Realm during the Paleocene-Eocene transition: Journal of Foraminifera research, v. 29, pp.37–57.

Pearson, P.N., Olsson, R.K., Huber, B.T., Hemleben, C., and Berggren W.A., (eds), 2006, Atlas of Eocene planktonic foraminifera. Cushman Foundation Special Publication, v. 41, pp. 1-513.

Perch-Nielsen, K., 1985, Mesozoic calcareous nannofossils in H. H. Bolli, J. B. Saunders, and K. Perch-Nielsen, eds. Plankton Stratigraphy. Cambridge University Press, pp. 329-426.

Raffi, I., Backman, J., Pälike, H., 2005, Changes in calcareous nannofossil assemblage across the Paleocene/Eocene transition from the paleo-equatorial Pacific Ocean: Paleogeography, Paleoclimatology, Paleoecology, v. 226, pp. 93–126.

Schulte, P., Scheibner, C., and Speijer, R., 2011, Fluvial discharge and sea-level changes controlling black shale deposition during the Paleocene–Eocene Thermal Maximum in the Dababiya Quarry section, Egypt: Chemical Geology, v. 285, pp. 167-183.

Speijer, R.P., Schmitz, B., and Luger, P., 2000, Stratigraphy of late Palaeocene events in the Middle East: Implications for low to middle-latitude successions and correlations: Journal of the Geological Society, London, v.157, pp.37-47.

Svensen, H., Planke, S., and Corfu, F., 2010, Zircon dating ties NE Atlantic sill emplacement to initial Eocene global warming: Journal of the Geological Society, London, v. 167, pp.433–36.

Tantawy, A. A., 2006, Calcareous nannofossils of the Paleocene-Eocene transition at Qena Region, Central Nile Valley, Egypt: Micropaleontology, v. 52, no. 3, pp.193-222.

Westerhold, T., Röhl, U., McCarren, H., and Zachos J., 2009, Latest on the absolute age of the Paleocene–Eocene Thermal Maximum (PETM): New insights from exact stratigraphic position of key ash layers + 19 and – 17: Earth and Planetary Science Letters, v.287, no. 3–4, pp. 412–419.

Zachos, J., Pagani, M., Sloan, L., Thomas, E., and Billups, K., 2001, Trends, rhythms, and aberrations in global climate 65 Ma to present: Science, v. 292, pp. 686–693.

Zachos, J.C., Röhl, U., Schellenberg, S.A., Sluijs, A., Hodell, D.A., Kelly, D.C., Thomas, E., Nicolo, M., Raffi, I., Lourens, L.J., McCarren, H., and Kroon, D., 2005, Rapid acidification of the ocean during the Paleocene–Eocene Thermal Maximum: Science, v.308, pp.161–1611.

Zachos, J.C., Wara, M.W., Bohaty, S., Delaney, M.L. and Petrizzo, M.R. 2003. A transient rise in tropical sea surface temperature during the Paleocene-Eocene Thermal Maximum: Science 302:1551–54.

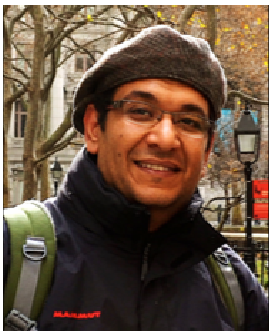

Hassan Khozyem, *is a lecturer in Geology department, Aswan Faculty of Sciences. He received his PhD (2013) at Lausanne University, Switzerland. Works mainly on geochemistry and sedimentology of Paleogene sediments in Egypt, India, and Spain. His research interests focus on global climatic and paleo environmental changes associated with warming events, with high-resolution bio-, and chemo-stratigraphy.*

Thierry Adatte *is Research Associate and head of the geochemistry and mineralogy sedimentary laboratory at the Geological Institute of the University of Lausanne, Switzerland. He received his Ph.D. in Mineralogy and Sedimentary Geology from the University of Neuchâtel, Switzerland. His research interests focus on global change associated with mass extinction events, high-resolution bio-, chemo- and sequence stratigraphy.*

Gerta Keller's *primary research centers on major catastrophes in Earth's history, including the biotic effects of meteorite impacts, major volcanic eruptions, rapid extreme climate changes, ocean anoxia and sea level changes associated with mass extinctions and rapid faunal turnovers. Her research integrates quantitative micropaleontology, paleoecology, stratigraphy, sedimentology, and stable isotopes in reconstructing paleoenvironments and exploring cause-effect scenarios.*

Abdel Aziz Tantawy *is a Professor of micropaleontology and Stratigraphy at the Department of Geology, Faculty of Science, Aswan University. He received his PhD (1998) at the University of South Valley. His research interests include the Cretaceous and Paleogene calcareous nannofossil stratigraphy and paleoecology, environmental changes across the stages boundaries (Cenomanian / Turonian, Campanian / Maastrichtian, Cretaceous / Tertiary, Paleocene / Eocene) in and outside Egypt.*

Jorge Spangenberg *holds a PhD in Geochemistry and is manager of the stable isotope and organic geochemistry laboratories at the Institute of Earth Science of the University of Lausanne. He has a special interest in bulk and compound-specific stable isotope approaches applied to geological issues and the environment. His current research topics include biogeochemical studies of Neoproterozoic and Permian-Triassic climate and environmental changes.*